Testing the Digital Imaging for Particle Analysis and Characterization (DIPAC) 100-L

August 10, 2011

CVO Sediment Laboratory

Introduction: The purpose of this report is to document the methods and results of testing the DIPAC-100L with fines sieved from material labeled "QAQC Lakewood silt/clay" and conventionally known as "AC spark plug dust". The goal of the testing was to document the repeatability, precision, and accuracy of size distribution and concentration measurements made with the most recent version of the DIPAC-100L and software. The most immediate goal of the DIPAC-100L research and development project is to develop a laboratory based instrument that can be used to measure the size distribution of very small amounts of fine material. Existing validated techniques for measuring the size distribution of fine material , such as the sedigraph or the pipette analysis, require substantially more material (approx 1.5g fine material minimum) than is commonly collected from a manageable volume of suspended sediment.

Methods: Two subsamples of QAQC Lakewood silt/clay reference material ("test dust") were scooped into a tared sedigraph cup, wetted, sonicated, and sieved at 63um. The sand fraction was then sized using the standard larger sieves and the fines were rinsed into a beaker. A larger subsample was scooped into a sedigraph cup, wetted, sonicated, sieved at 63um, and the fines were analyzed in the sedigraph. The resulting distribution was used for comparison with the results from the optical analysis.

The DIPAC-100L has two separate channels for imaging particles at low and high magnification. Only the high magnification channel was used in this test. The low magnification channel is designed for imaging analysis of sands; the high magnification channel is designed for imaging analysis of fines. Sizing sands can also be accomplished with a sieve analysis, so the current thrust of the research focuses on the high magnification channel.

The DIPAC-100L was set up in a vertical configuration (Figure 1). The vertical configuration ensures that all particles flow past the imaging area. In horizontal configuration the flow is not always sufficient to move the particles up the inlet ramp into the imaging area. The sample is added to a funnel, which is connected by tygon tubing to a 0.125"i.d. metal inlet fixture. The sample is then pumped through the channel, where it is illuminated by a flash from a Volpi IntraLED 2020 LED light controlled by a Gardasoft PP520F strobe controller and imaged with a DMK41BU02 camera from TheImagingSource. The camera and strobe controller are triggered by an Arduino Duemilanove. The lenses on the camera are Navitar Precise Eye 2.0X lens attachment with a 2.0x Adapter. The sample is then pumped through the outlet fitting, which starts at 0.125"i.d. and then abruptly narrows to 0.071"i.d. to allow connection with the Tygon 95609-42 (0.0812" i.d.) tubing. The narrower tubing allows us to use the Masterflex C/L pump which has a low flow rate, giving us more control over the velocity of the flow in the channel than when we used the wider tubing and the Masterflex L/S pump through the whole setup. The abrupt transition in cross-sectional area at the outlet is undesirable and slated for revision in subsequent versions of the flow cell. The sample is pumped past the outlet and then through the pump and into the outlet receptacle. The pump draws the sample through the imaging area. A simple pulse dampener consisting of a t-junction with an air pocket trapped above the main flow functions to reduce the pressure extremes caused by the pump peristalsis. The pulse dampener is below the outlet and above the pump. The pump is laid on its side to ensure that the flow path is sloped downward over its entire length. Experience has shown that pumping particles up a slope leads to a buildup of particles in the upslope

areas even when the pump speeds are high, so the continual downsloping is a crucial element of the overall configuration of the system

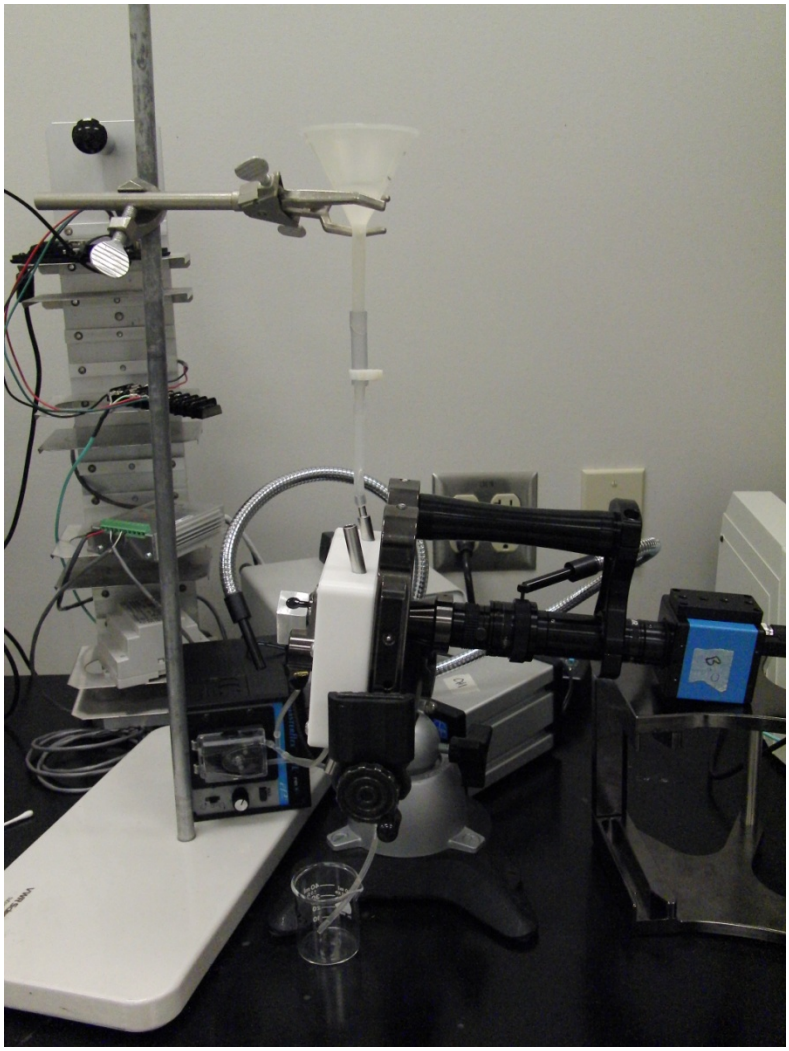

Figure 1: The physical setup of the DIPAC-100L for testing

At the beginning of the set of runs, I experimented with the aperture, lighting, and focus settings to produce the best quality images of this test dust. The aperture is variable width, manual control, so it is not possible to determine its exact width, but it is quite narrow. Increasing the aperture increases the depth of field but decreases the light level and the resolving power in the range of the finest particles. The lighting is set to 250% brightness (1.5A) and the minimum pulse width (3us). Oscilloscope traces of the electrical signal coming out of the strobe controller indicate that the electrical pulse is in fact closer to 8us in duration. The controller is wired directly to the LED in the Volpi light. However, the rise and fall times of the LED under this current are unknown. It is possible that the pulse is longer as the LED fall time could be in the microseconds range. Designing a photodiode sensor to measure the precise

duration of LED lighting under this set of conditions is planned for the next phase of the project. Once I set the aperture, focus, and lighting for this set of runs I did not change them for any subsequent tests.

To measure a sample, I first filled the tubing and flow cell with DI water, pumped at maximum pump speed. At max speed, it was possible to pull through the bubble that formed at the bottom of the funnel where it connected to the wide tubing when the funnel was filled. It was necessary to pinch the tubing and release it multiple times, or even run the pump backward to clear the bubble. At lower pump speeds, the flow rate was insufficient to completely fill the tubing above the flow reducer, so a bubble formed in the wide tubing and the reducer.

When the tubing was full of blank DI that ran clear of particles in the live image view, I shut off the pump and entered the information for the run into the software. I then set the pump to approximately half speed (point marked on dial on pump), turned on the pump and immediately started the imaging. The half speed was chosen because it generates enough flow to move the particles through the tubing while not moving them so fast that velocity blurring is visible in the images.

Images were taken 303ms apart because earlier analysis of high speed video of the pump rotation indicated that this would take an image precisely every two cycles of opening and closing the tubing from the peristaltic rollers in the pump at this speed. It was important to synch the imaging timing to the timing of the flow fluctuations in the tubing so that a uniform volume of sample passed the imaging area during each sampling interval.

As the clean DI flowed through the cell, I vigorously stirred the beaker of test dust, which I had recently sonicated. I withdrew either a single 1ml subsample or 5 1ml subsamples from the stirred suspension with a transfer pipette and added them to the DI water in the funnel. I then rinsed down the sides of the funnel and began stirring the sides of the funnel with a teflon stick. It was important to use the teflon stick because earlier analysis in which a rubber policeman was used showed that the rubber policeman contaminated the sample with rubber particles. As the funnel drained, I rinsed down the sides of the funnel with DI a few more times. When the sample was at the top of the inlet fitting I stopped the images and then let the pump clear the line into the tared outlet beaker.

The outlet rinsate was collected in a tared 50ml beaker at the outlet of the pump. Immediately after the sample was fully pumped into the outlet beaker, I weighed the beaker again. The difference between the gross and tare weights in grams was considered equivalent to the volume of sample for computing the concentration by filtration. I then filtered the sample into a tared crucible, dried it, cooled it in the desiccator, and weighed it back.

After I weighed back the sample beaker, I flushed the system into a separate, tared, 150ml beaker. I flushed the system at the maximum pump speed in order to clear any remaining sample from the hoses. While the system was flushing, I added DI, and rinsed down the sides of the funnel extensively. As the system was flushing, I watched the live image display. My observation of the live display was that few particles were left above the imaging area after the run. Most of the material that rinsed out in the flush came from below the imaging area, almost certainly from the outlet fitting, which has an abrupt

hydraulic jump that can accumulate particles when the pump speed is low. I collected the rinsate from the flush, weighed back the beaker, filtered the rinsate, and weighed it back in a similar manner to the sample material. When the live display showed a clear image for a sufficient time to give me confidence that the system was clean, I cleared any remaining bubble from the flow reducer and shut off the pump, leaving the system full of clear DI and ready for the addition of the next sample.

In some cases, I attempted to recycle the sample material directly into the funnel and re-measure the same sample multiple times. My purpose in this was to see what how well I could replicate the results from a single sample. However, this was unsuccessful because I could not clear the bubble at the flow reducer above the inlet without the max speed flush in between samples. The sample still flowed through the system when the bubblewas present, but its presence affected the hydraulics of the system in unpredictable ways. I did not use the results of the second or third runs of the same sample for comparison to other runs that were not recycled. The first run in a set of recycled samples was taken under directly comparable conditions to the other samples that were not recycled, so those runs were included in the final analysis.

I tested four runs in which I added approximately 1ml of the suspension of fines, and four runs in which I added approximately 5ml of the suspension of fines. The withdrawals were made with a transfer pipette, and so were inherently imprecise volumes (Table 1).

I used the image extraction algorithm in ParticleSeparation.Objects.Run.vb, SVN revision 40 to extract the blobs from the images. In brief, the algorithm extracts edges from the original image, normalized to the background image. It then extracts filled blobs from these edges, applies a halo around the high confidence blobs, and erases the high confidence blobs from the image by replacing the blobs and their halo with the background signal when the grayscale in the halo is lighter than some threshold darkness, set by the user as a number of standard deviations darker than the background signal. If the background is dark, which it in the case of all these images, the resulting image with the high confidence blobs erased is then contrast stretched, another set of edges are found, the blobs are extracted from the found edges, and those blobs are erased. The contrast-stretched image is then re-extracted a third and final time with tweaked settings that allow it to find ever fainter and blurrier particles. At each blob extraction, only blobs at least a user-definable grayscale value darker than then mean background grayscale are kept, to prevent extraneous blobs from being included. A final watershed separation separates touching particles that have two distance nodes in their binary shape. After watershed separation, a final blob extraction is performed, the shape parameters are calculated, and the information is stored in a MySQL database. No specific minimum area criterion is set in the blob extraction, however, a morphological erode/dilate sequence is used to clean up edges that did not close into filled blobs. This effectively limits the size of found blobs to those that can survive a 1-pixel erosion, or a 9-pixel square. A 9-pixel square corresponds to a 1.96um particle. However, the precise size of the minimum area depends somewhat on the shape of the blobs that are eroded. At the current optical setting it is difficult to resolve particles in the 1.96um range because of the aperture.

After the blobs are extracted, the blob area is used to classify the size of the blob. The area in pixels is converted to the corresponding area in square microns. The diameter of a circle that has an equivalent

area is used as the particle diameter, and the volume of a sphere with the radius corresponding to that diameter is used as the particle volume. The particle volume is converted to mass using an assumed density of 2.65g/cm3. The density assumption does not affect the size distribution, but does affect the concentration measurements. The total mass of all particles is summed and divided by the total sampled volume to compute the concentration. The sampled volume is the image length times the image width times the channel depth (0.006”(152um)) times the number of images. The size distribution is constructed by summing the masses of all particles with a diameter less than the bin size. The mass in each bin is then divided by the total mass to get the percent finer than the bin size.

The calibration used to convert a pixel to its corresponding world units is based on analysis of a test run of 6um polystyrene beads (Polysciences, Inc. Cat #24293) taken at the same brightness, focus, and aperture settings as the runs of the test dust. The beads have a known mean diameter of 6.017 ± 0.168um. There were 120 images in the test run, and a total of 3042 particles were extracted. There was a strong central tendency in the distribution of the areas of the extracted blobs (Figure 2). Larger blobs are either beads that are stuck to each other or minor amounts of contaminating dust. Smaller particles are either minor amount of small dust particles or 6um beads that intersected the edge of the image.

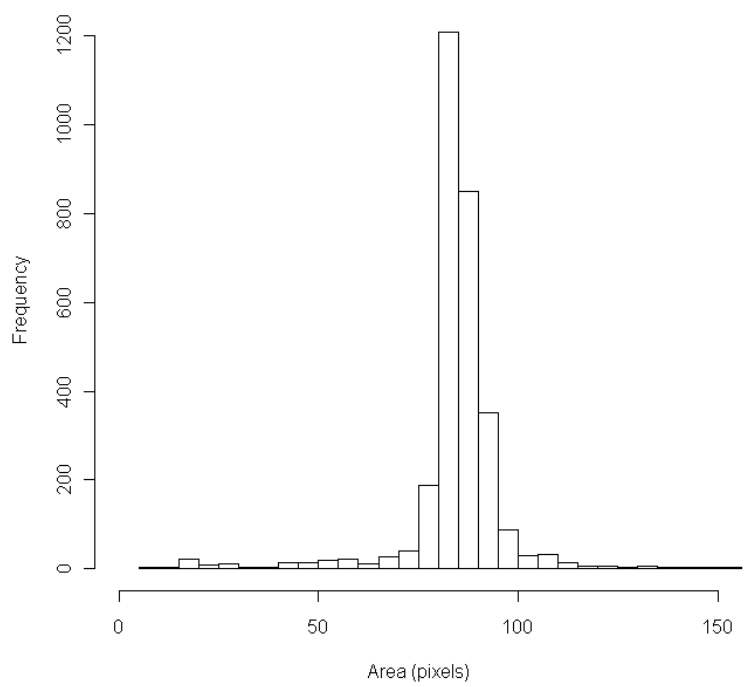

Figure 2: Histogram of the areas in pixels of the 6um test beads recovered in a run of 120 images. The strong central tendency in the 80-90 pixel range represents the detections of the uniformly sized beads.

Assuming that the most frequently detected particle area (85 pixels) represents a 6.017um bead, the corresponding pixel to micron conversion is 1.728pixels/um, equivalent to a 0.578um length of the side

of each pixel. Applying this calibration to the areas of the 6um test beads results in a distribution that is very well matched to the target distribution (Figure 3).

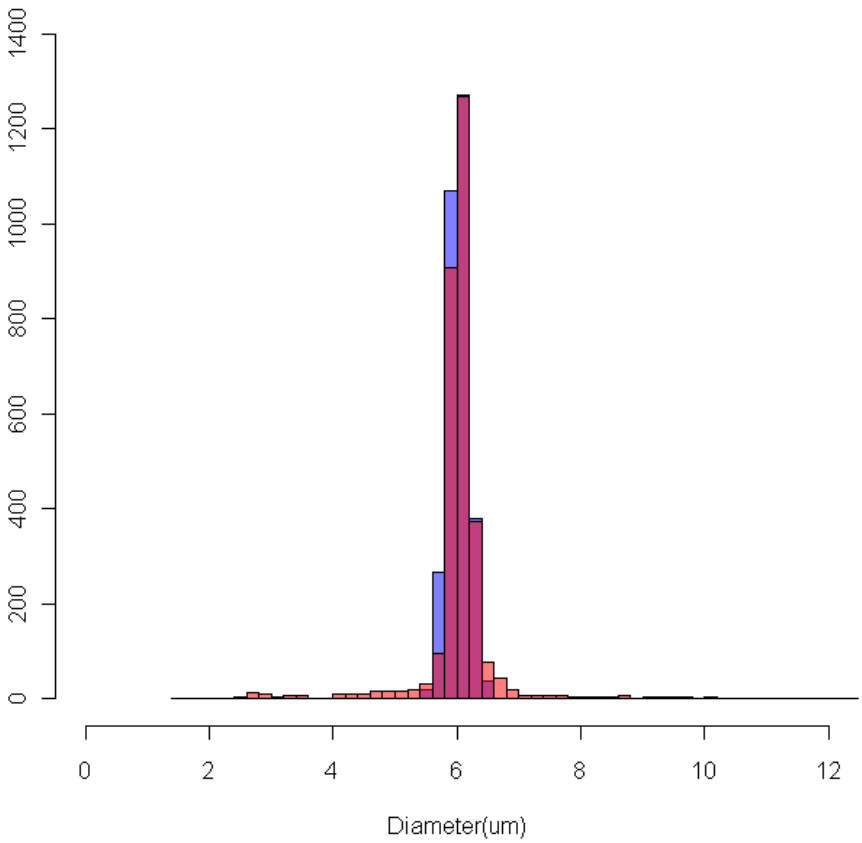

Figure 3: Measured distribution (red) and target distribution (blue) of the diameters of 6um test beads after calibration. Purple bars are areas of overlap between the red and blue bars. There is strong agreement between the target and measured size distributions.

The results of the 6um bead tests can also be used to determine if there is size distortion at the edges of the images. If there was distortion in the sizes at the edges of the images, then there would be a trend in measured particle diameters across the image. No such pattern was detected (Figure 4). Although this calibration technique is not able to assess the full range of sizes measured in the DIPAC it is internally consistent. Next phases of the research will aim to develop a calibration target to assess the validity of this calibration over the range of expected sizes.

The calibration from the 6um bead tests was used to convert the area in pixels of the extracted blobs to the corresponding particle diameters. The final size distribution was then compared to the size distribution from the sedigraph to assess the precision and accuracy of the measurement in the DIPAC. We do not expect the sedigraph results to agree perfectly with the DIPAC results because the sedigraph is based on settling velocity. Nonetheless, the results should be comparable. We also compared the

concentration measured in the DIPAC to the concentration measured by filtering the rinsate from each sample and its corresponding flush.

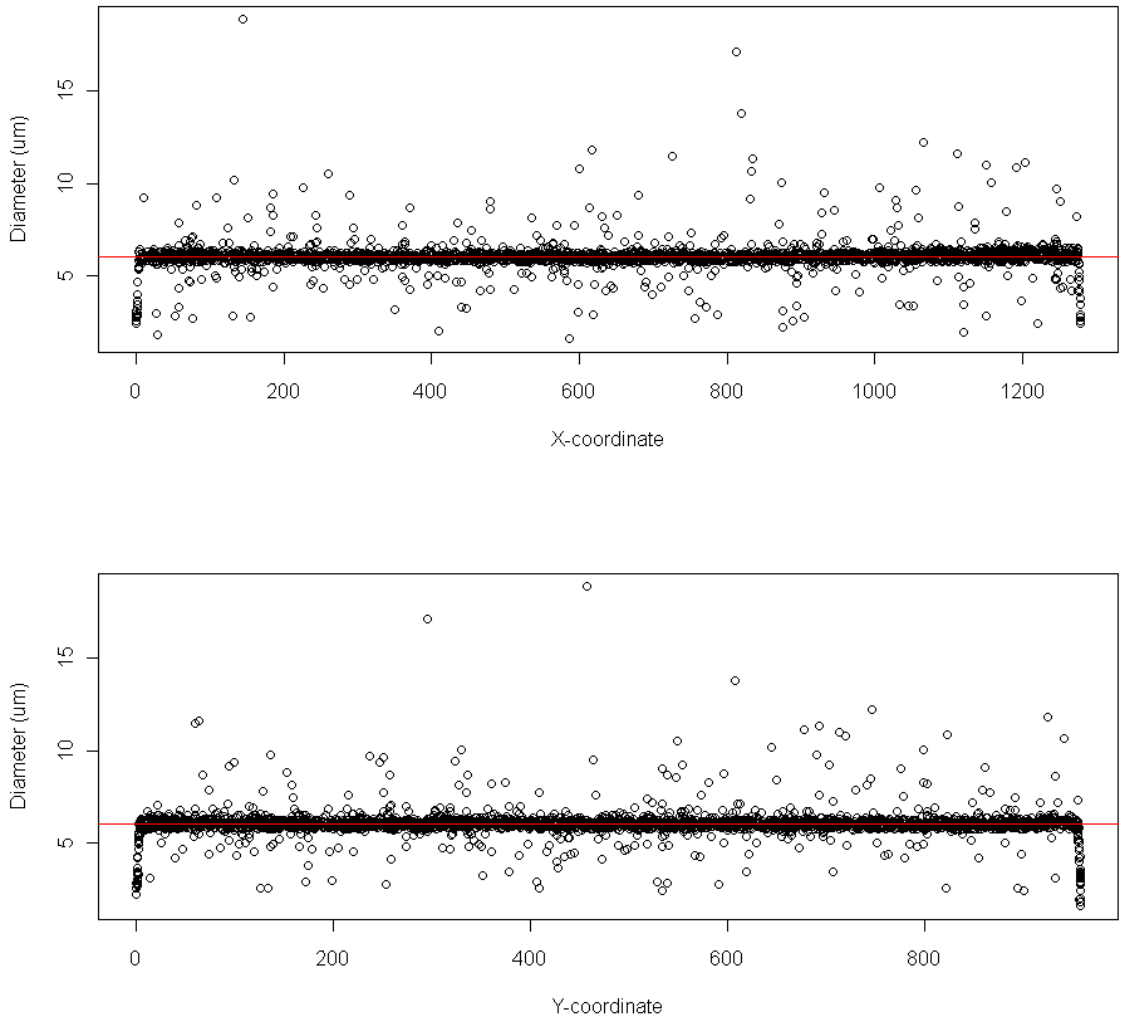

Figure 4: Measured diameters of 6um test beads did not change across the images in either the x direction or the y direction, indicating that there is no detectable spherical aberration in the lenses. Decreases in diameter at the edges of the images are due to particles intersecting the edge of the image. The red lines are drawn at the mean diameter of 6.017um.

name	ml suspension added	Volume in run (ml)	Mass in run (g)	Mass in flush (g)	Conc. by filtration (mg/L)	No. of images	No. of part. found	Measured conc. In DIPAC (mg/L)
1mlhalf1	1	42.4	0.0031	0.0009	93±24	563	18457	204
1mlhalf3	1	37.3	0.0020	0.0008	75±27	424	15852	182
1mlhalf4	1	45.0	0.0021	0.0012	73±22	558	18624	165
1mlhalf5a	1	39.2	0.0019	0.0010	74±26	451	17405	187
5mlhalf6a	5	35.9	0.0097	0.0018	320±28	453	74836	840
5mlhalf7	5	47.3	0.0099	0.0027	266±21	653	77375	662
5mlhalf9	5	50.0	0.0154	0.0032	372±20	602	115494	1027
5mlhalf10	5	45.1	0.0119	0.0027	324±22	602	94921	800

Table 1: Characteristics of the seven runs used in this analysis. 1mlhalf2 was taken at a different aperture setting and 5mlhalf8 had a bubble in the flow reducer that I did not detect until later in the run.

Results: The size distribution measured in both 5ml and 1ml subsamples of the suspension of test material agreed with the results of the sedigraph to within 10% down to 6um (Figures 5, 6). Below 6um, the results diverged due to the inability of the DIPAC to resolve particles in the <3um range. The variability among runs is greater in the 1ml runs, as expected when fewer particles are measured. The variability among runs incorporates the variability from the DIPAC analysis as well as the variability due to taking very small subsamples of fine particles in suspension.

There was a strong correlation between the concentration measured in the DIPAC and the concentration measured by filtration (spearman's rho=0.952, p=0.001) (Figure 7). The ratio between the DIPAC concentration and the concentration by filtration was 2.46+/- 0.18, indicating that the DIPAC is consistently measuring the concentration high by a factor of approximately 2.5.

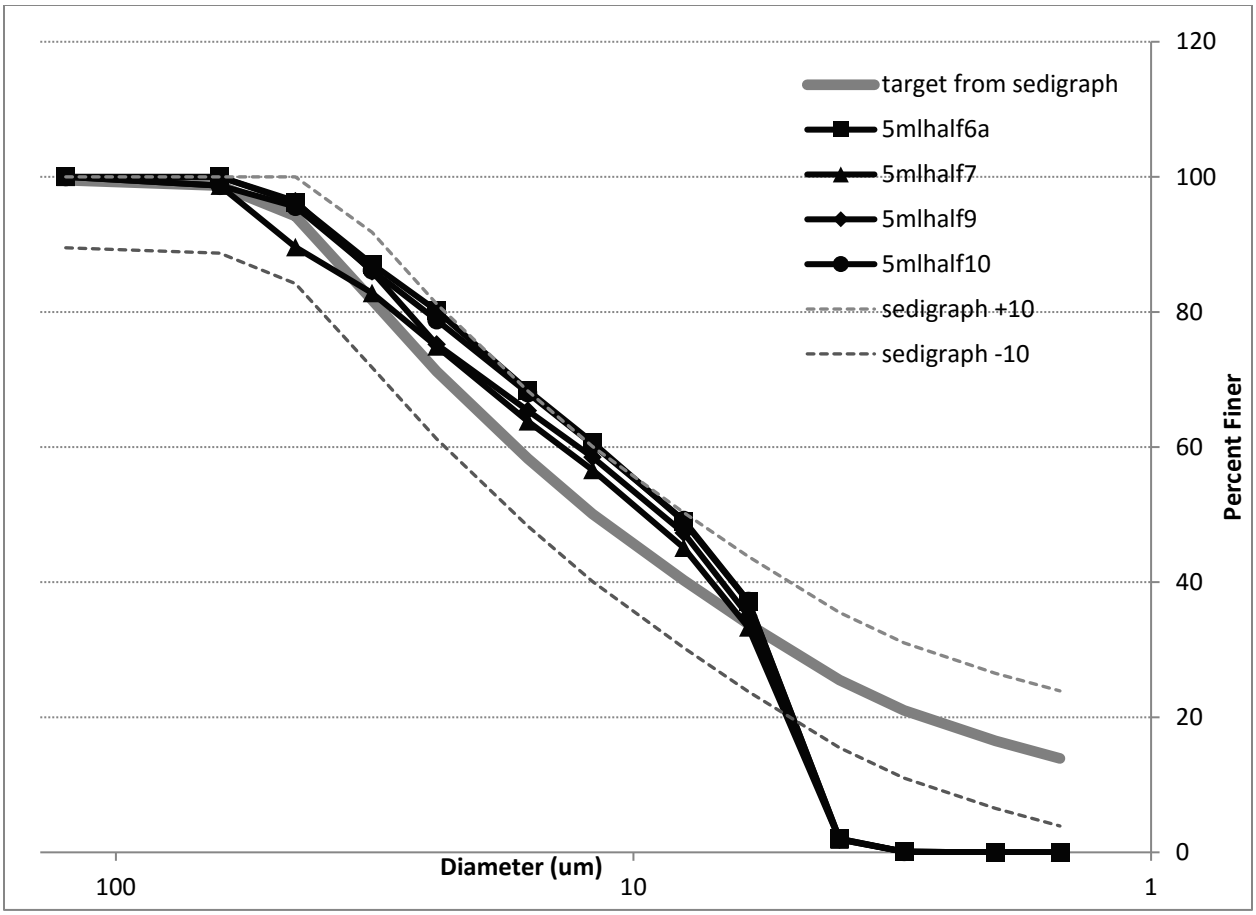

Figure 5: Size distributions measured in four 5ml subsamples of a suspension of fines sieved from AC spark plug dust. The target distribution was measured on a separate, larger subsample in the sedigraph. Sizes are reported at 125, 63, 45, 32, 24, 16, 12, 8, 6, 4, 3, 2, 1.5, and 1um.

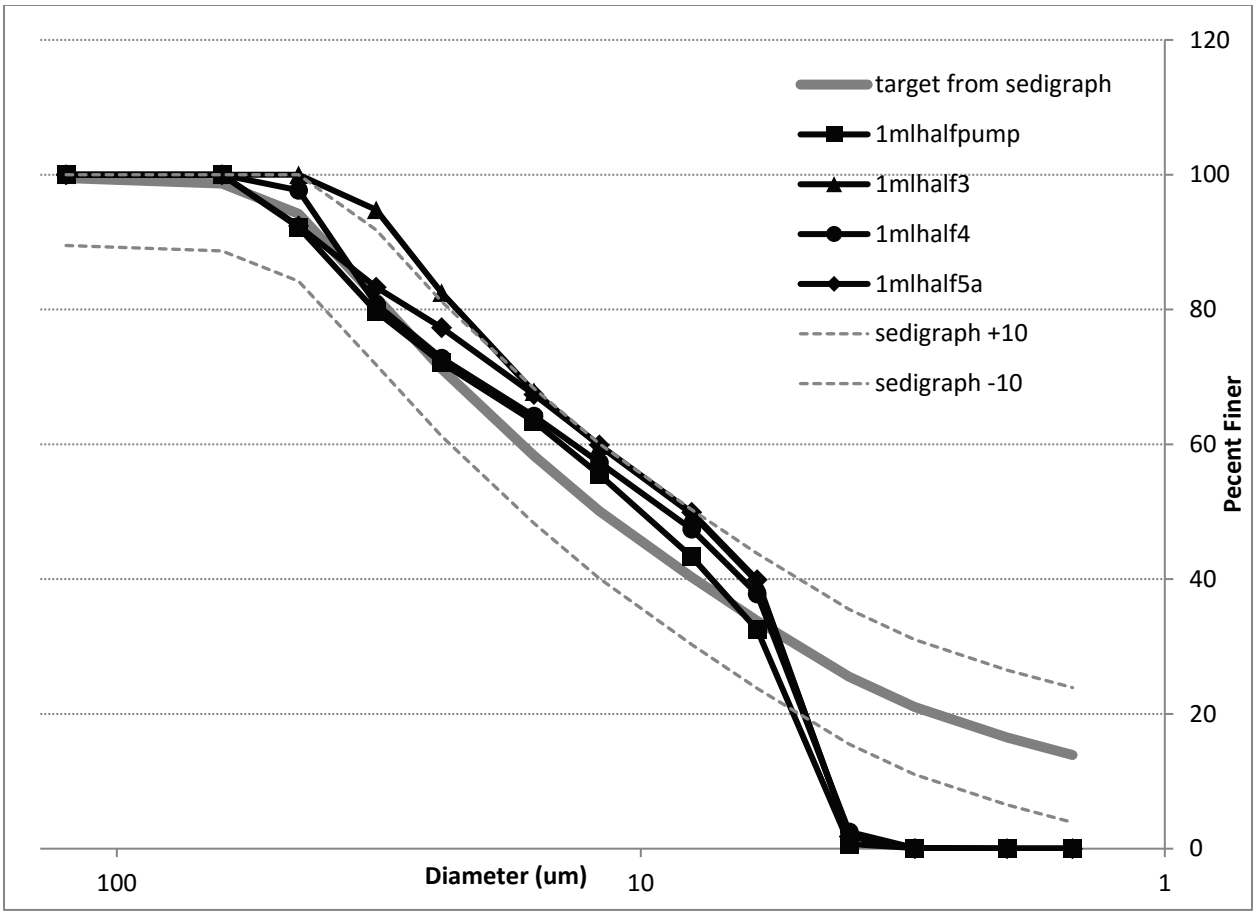

Figure 6: Size distributions measured in four 1ml subsamples of a suspension of fines sieved from AC spark plug dust. The target distribution was measured on a separate, larger subsample in the sedigraph. Sizes are reported at 125, 63, 45, 32, 24, 16, 12, 8, 6, 4, 3, 2, 1.5, and 1um. The variability between subsamples is less for the 5ml subsamples (Figure 5) than for the 1ml subsamples, as expected.

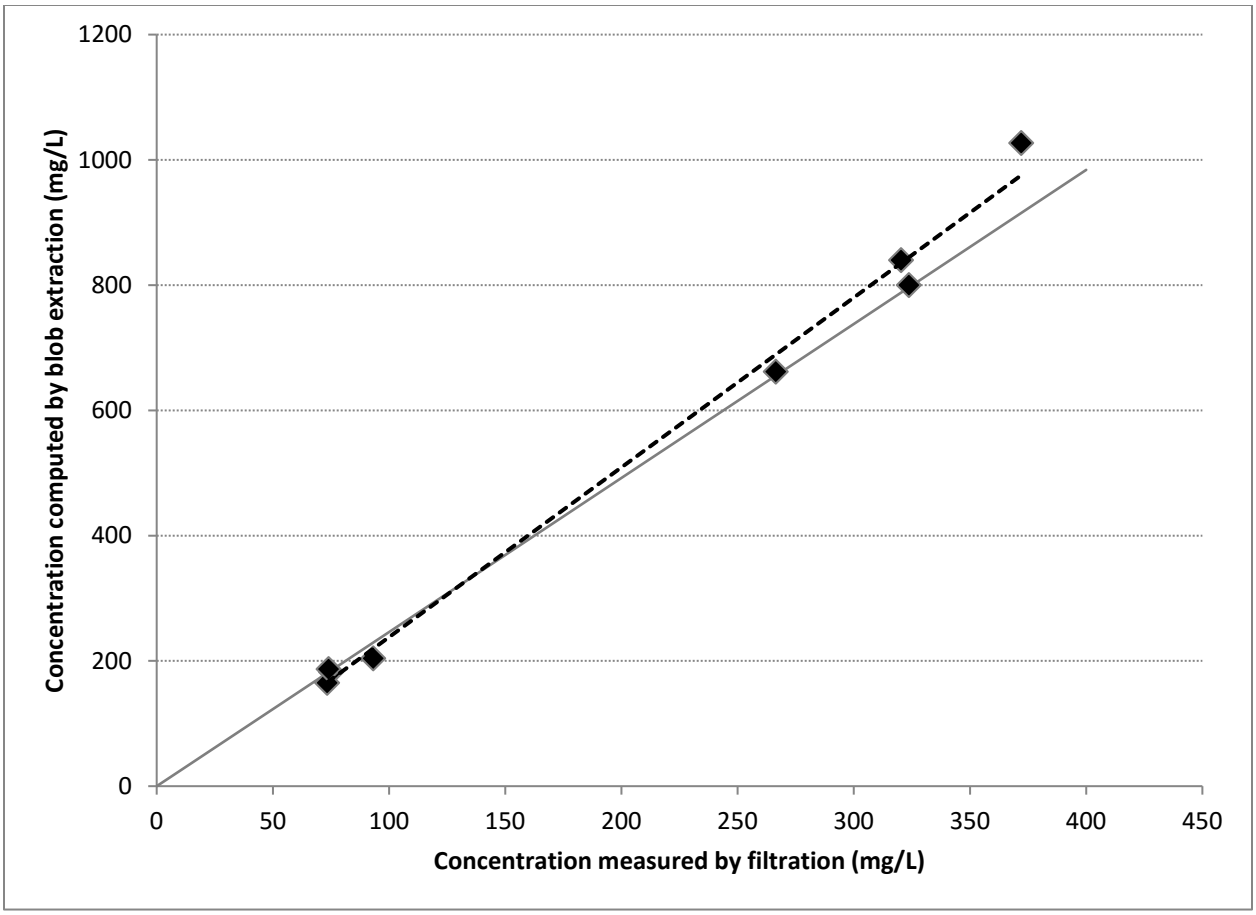

Figure 7: Relationship between the DIPAC concentration and the concentration measured by filtration for each of 8 test runs (spearman's rho = 0.952, p=0.001). Dashed line is the best fit line and the solid gray line is a line with a slope of 2.46, the mean ratio between the two measurements of concentration.

Discussion: The results indicate that the precision and accuracy of the DIPAC in this configuration are sufficient to measure particle size distributions of small amounts of fine sediment down to 6um (Figures 5,6). The accurate measurement at 6um indicates that we are detecting a sufficient amount of the mass finer than 6um, effectively the 4um-6um fraction. Below 4um, we are not detecting enough of the mass, due to limits of the resolving power of the lenses, the aperture, the lighting, and the noise removal in the blob extraction algorithm. We are working to continually improve the lighting, lenses, and software to drive the minimum detectable particle size down, with an eventual goal of 2um.

The DIPAC analysis detected a finer distribution than the sedigraph (Figures 5, 6). This could be due to the relatively low number of large particles measured in the DIPAC. Future runs are intended to set a minimum number of detections of large particles as part of the QA/QC for the instrument. Particle counts can be increased by increasing the concentration of the sample, increasing the speed of imaging, and increasing the duration of imaging. Alternatively the minor differences in the DIPAC and sedigraph distributions could be due to natural discrepancies between size distributions based on fall diameter and those based on direct measurement of size.

It is unclear why the concentration is over estimated in the DIPAC by such a consistent ratio. Further tests, at a wider range of input concentrations, need to be conducted in order to confirm the relationship.

The results presented here attempt to capture the realized error in the results from the DIPAC; further analysis is needed to quantify the theoretical error and determine the best precision possible for the system under a range of conditions. We should be able to use Poisson statistics to predict the theoretical error in the particle counts in each size class, and use that to estimate the error in the size distributions under different conditions.

We also need to incorporate our idea of the precision and accuracy of the measurements of the individual particles into our error model for the size distribution. The precision and accuracy of the size measurements depend on the quality of the blob extraction algorithm, the quality of the optical conditions, and the quality of the pixel-to-world-units calibration. We are continually working to improve the software and the optics, and our next steps include developing a custom calibration target to define the pixel-to-world-units calibration more precisely over a wider range of target sizes.

Overall, the results strongly indicate that we can use the DIPAC in its current configuration to reliably measure the size distribution of very small samples of fine sediments, down to 6um. There are two advantages to the DIPAC over current technology. First, it can handle very small amounts of material, allowing hydrologists to get size results for very light suspended samples. Second, the DIPAC provides more information about the shape and size of particles than available from settling velocity measurements. Eventually we hope to refine our estimates of particle diameters and volumes based on particle shape, and provide end users information about the shapes of the particles. Testing and refinement is ongoing, but these results indicate that the DIPAC can work in its current configuration and has a good probability of eventually going on to be a validated USGS particle sizing technique.